Analyzing power formula and application to low energy nuclear reactions

M. Tanifuji
Department of Physics, Hosei University, Tokyo 102, Japan

H. Kameyama
Chiba-Keizai College, Chiba 263, Japan

(Received 12 February 1999; published 6 August 1999)

General formulas of analyzing powers in nuclear reactions are derived in a model-independent way, decomposing the analyzing powers by the rank of tensors in the spin space by the invariant-amplitude method. The validity of the formulas is examined in low energy reactions, the ^{3}He$(\vec{d},p)^4$He reaction at the 430-keV resonance and ^{1}H$(\vec{d},\gamma)^3$He reactions at energies below 80 keV, for which the formulas reproduce experimental data very well. The analyses clarify the following. The former reaction occurs mainly due to tensor interactions with incident S waves while P wave corrections by spin-orbit interactions have indispensable contributions to the analyzing powers. The data of the latter reaction are explained by the vector transition amplitudes in the spin space. The formulas predict the angular distribution of the analyzing power T_{kq} (k=even) to be similar to $P_k^q(\cos\theta)$ for incident S waves when Q values are finite. [S0556-2813(99)05908-7]

PACS number(s): 24.70.+s, 24.10.−i, 24.30.−v, 25.10.+s

I. INTRODUCTION

Investigations of polarization observables in nuclear reactions—for example, of analyzing powers for polarized beams—provide substantial information on nuclear spin-dependent interactions as well as underlying reaction mechanisms. In practice, possible spin-dependent interactions take part together in a reaction and their effects are mixed up with each other in the observables, resulting in difficulties in finding of the contributions of each spin-dependent interaction. To identify the effect of a particular spin-dependent interaction on the observable, it will be useful to decompose reaction amplitudes into spin-space tensors, because spin-dependent interactions—for example, spin-orbit interactions, so-called tensor ones, etc.—are classified, according to their tensorial character in the spin space, as the vector, the second-rank tensor, and so on, and thus in such decomposition each component of the amplitude is tagged by the corresponding spin-dependent interaction. When the observable is calculated by the tagged amplitudes, one will find the effect of the relevant spin-dependent interaction on the observable in an easy way. The decomposition of the amplitudes has been performed earlier [1,2] with success to clarify the role of the individual spin-dependent interaction in the reaction mechanism [1–9].

To perform such kinds of analyses more efficiently, it will be worthwhile to decompose the polarization observable itself by the tensor rank in the spin space, taking a step forward from the amplitude decomposition. This will allow us to extract directly the contribution of a particular spin-dependent interaction from the observable. For that purpose, we will derive the formula for each component of the observable in such decomposition—for example, for analyzing powers. The extension to other observables is quite easy. The theory is developed by the invariant-amplitude method [1], where the geometrical parts of the T-matrix elements are simply calculated due to the decomposition and the physical parts are described by the invariant amplitudes which are designated by the tensor rank. More details of the method are given later. The formulas are model independent, although the final state is restricted to two-body ones, and thus will be widely applicable.

In the next section, we will derive the formulas of the cross section and the analyzing powers. They are general but are inconvenient to handle. For practical convenience, we will give their explicit forms, specializing the analyzing power to the vector one and the tensor ones, and limiting the tensor rank to 1 and 2. The validity of the present formulas is not limited by the incident energy of the reaction. However, the application is very simple in low energy reactions because of a small number of the effective partial waves. Since the explicit forms are different between parity-unchanged reactions and parity-changed ones, we will choose examples of the application, by one for each case, i.e., the ^{3}He$(\vec{d},p)^4$He reaction at the 430-keV resonance for the former and ^{1}H$(\vec{d},\gamma)^3$He reactions at the center-of-mass energies below 80 keV for the latter, where the photon is treated as a 1^- particle. The former reaction is well known to give a measure of the polarization of the deuteron and is employed in experiments as an analyzer [10]. This requires refined measurements and analyses of the analyzing powers. Also, the role of the spin-dependent interactions has not been clarified. The latter reaction has recently gained attention because of astrophysical interests and one needs detailed information on the reaction mechanism [11].

II. DERIVATION OF FORMULAS OF THE CROSS SECTION AND ANALYZING POWERS

Let us consider a reaction $a+A\rightarrow b+B$. The analyzing power T_{kq} for the polarized projectile a is given in Ref. [12] as

$$T_{kq}=\frac{1}{N_R}\mathrm{Tr}(\boldsymbol{M}\tau_{kq}\boldsymbol{M}^{\dagger}), \tag{2.1}$$

with

$$N_R=\mathrm{Tr}(\boldsymbol{M}\boldsymbol{M}^{\dagger}), \tag{2.2}$$

where $\boldsymbol{M}$ is the T matrix of the reaction and τ_{kq} is the spin operator of the projectile with the rank k and the z component q. The matrix element of τ_{kq} is given by

$$\langle s_a\nu_a'|\tau_{kq}|s_a\nu_a\rangle=\hat{k}(s_a k\nu_a q|s_a\nu_a'), \tag{2.3}$$

where $s(\nu)$ denotes the spin (z component).

First we will introduce the decomposition of the reaction amplitude into the spin-space tensors, by which we will construct the formula of analyzing power using Eq. (2.1). Expand $\boldsymbol{M}$ into the spin-space tensor $\boldsymbol{S}_{K\kappa}$, where $K(\kappa)$ is the rank (z component) of the tensor,

$$\boldsymbol{M}=\sum_K \boldsymbol{M}_K, \tag{2.4}$$

with

$$\boldsymbol{M}_K=\sum_\kappa (-)^{\kappa}\boldsymbol{S}_{K-\kappa}\boldsymbol{R}_{K\kappa}, \tag{2.5}$$

where $\boldsymbol{R}_{K\kappa}$ is the tensor in coordinate space. The matrix element of $\boldsymbol{M}_K$ describes the reaction amplitude due to the interaction of the rank K in the spin space, which includes higher order terms of any interaction as long as they have the tensorial property of rank K. Effects of D states of the internal motions of the related nuclei are included in the amplitude of $K=2$. Using Eq. (2.4),

$$\mathrm{Tr}(\boldsymbol{M}\tau_{kq}\boldsymbol{M}^{\dagger})=\sum_{KK'}\mathrm{Tr}(\boldsymbol{M}_{K'}\tau_{kq}\boldsymbol{M}_K^{\dagger}). \tag{2.6}$$

The matrix element of $\boldsymbol{M}_K$ is given by the invariant-amplitude method [1],

$$\langle \nu_b\nu_B;\boldsymbol{k}_f|\boldsymbol{M}_K|\nu_a\nu_A;\boldsymbol{k}_i\rangle=\sum_{s_i s_f}(s_a s_A\nu_a\nu_A|s_i\nu_i)(s_b s_B\nu_b\nu_B|s_f\nu_f)(-)^{s_f-\nu_f}(s_i s_f\nu_i-\nu_f|K\kappa)$$
$$\times\sum_{l_i=K-K}^{K}[C_{l_i}(\hat{\boldsymbol{k}}_i)\otimes C_{l_f=\overline{K}-l_i}(\hat{\boldsymbol{k}}_f)]_\kappa^K F(s_i s_f K l_i;\cos\theta), \tag{2.7}$$

where $\boldsymbol{k}_i$ ($\boldsymbol{k}_f$) denotes the a-A (b-B) relative momentum in the incident (outgoing) channel, θ is the relative angle between $\boldsymbol{k}_i$ and $\boldsymbol{k}_f$, and C_{lm} is related to Y_{lm} as usual. The quantity $\overline{K}$ is K for $K=$even and $K+1$ for $K=$odd when the parity is unchanged by the reaction, $\pi(a)\pi(A)=\pi(b)\pi(B)$, and $\overline{K}$ is $K+1$ for $K=$even and K for $K=$odd when $\pi(a)\pi(A)\neq\pi(b)\pi(B)$, as shown in the Appendix of Ref. [1]. In the derivation of Eq. (2.7), the matrix element of $\boldsymbol{S}_{K-\kappa}$ is calculated by the Wigner-Eckart theorem, where the geometrical part is given by the Clebsch-Gordan coefficients in the equation. The geometrical part of the matrix element of $\boldsymbol{R}_{K\kappa}$ will be represented by $[C_{l_i}(\hat{\boldsymbol{k}}_i)\otimes C_{l_f}(\hat{\boldsymbol{k}}_f)]_\kappa^K$ since the matrix element is a tensor constructed of ordinary-space vectors and we have only two such vectors, $\boldsymbol{k}_i$ and $\boldsymbol{k}_f$, after the integration over the coordinate variables. The physical parts of both matrix elements are included in the amplitude $F(s_i s_f K l_i;\cos\theta)$, which is designated by the relevant tensor rank K and is a function of the center-of-mass energy. We call $F(s_i s_f K l_i;\cos\theta)$ the invariant amplitude because it is invariant under rotations of the coordinate axes. The quantity l_i (l_f) gives the orbital angular momentum in the incident (outgoing) channel when the θ dependence of $F(s_i s_f K l_i;\cos\theta)$ is neglected. As will be discussed later, the θ dependence yields additional angular momenta.

After some Racah-algebraic calculations, Eq. (2.7) gives

$$\mathrm{Tr}(\boldsymbol{M}_{K'}\tau_{kq}\boldsymbol{M}_K^{\dagger})=(-)^k\hat{k}\sum_{s_i s_i' s_f}\hat{s}_i\hat{s}_i'\hat{s}_a W(s_i' s_A k s_a;s_a s_i)W(k s_i K' s_f;s_i' K)\hat{K}\sum_\kappa(kKq\kappa|K'\kappa')\sum_{l_i}[C_{l_i}(\hat{\boldsymbol{k}}_i)$$
$$\otimes C_{l_f}(\hat{\boldsymbol{k}}_f)]_\kappa^{K*}\sum_{l_i'}[C_{l_i'}(\hat{\boldsymbol{k}}_i)\otimes C_{l_f'}(\hat{\boldsymbol{k}}_f)]_{\kappa'}^{K'}F^*(s_i s_f K l_i;\cos\theta)F(s_i' s_f K' l_i';\cos\theta), \tag{2.8}$$

which satisfies

$$\mathrm{Tr}(\boldsymbol{M}_K\tau_{kq}\boldsymbol{M}_{K'}^{\dagger})=(-)^k\,\mathrm{Tr}(\boldsymbol{M}_{K'}\tau_{kq}\boldsymbol{M}_K^{\dagger})^*. \tag{2.9}$$

To transform $C_l(\hat{\boldsymbol{k}})$ and $C_{l'}(\hat{\boldsymbol{k}})$ in Eq. (2.8) into single $C_L(\hat{\boldsymbol{k}})$, we will use the following relations:

$$\sum_{\kappa}(kKq\kappa|K'\kappa')[C_{l_i}(\hat{\boldsymbol{k}}_i)\otimes C_{l_f}(\hat{\boldsymbol{k}}_f)]^{K*}_{\kappa}[C_{l'_i}(\hat{\boldsymbol{k}}_i)\otimes C_{l'_f}(\hat{\boldsymbol{k}}_f)]^{K'}_{\kappa'}=(-)^{\bar{K}}\hat{K}'\hat{k}^{-1}[[C_{l_i}(\hat{\boldsymbol{k}}_i)\otimes C_{l_f}(\hat{\boldsymbol{k}}_f)]^{K}\otimes[C_{l'_i}(\hat{\boldsymbol{k}}_i)\otimes C_{l'_f}(\hat{\boldsymbol{k}}_f)]^{K'}]^{k}_{q} \tag{2.10}$$

and

$$[[C_{l_i}(\hat{\boldsymbol{k}}_i)\otimes C_{l_f}(\hat{\boldsymbol{k}}_f)]^{K}\otimes[C_{l'_i}(\hat{\boldsymbol{k}}_i)\otimes C_{l'_f}(\hat{\boldsymbol{k}}_f)]^{K'}]^{k}_{q}$$
$$=\hat{K}\hat{K}'\sum_{L_iL_f}\hat{L}_i\hat{L}_fU\begin{pmatrix} l_i & l_f & K\\ l'_i & l'_f & K'\\ L_i & L_f & k\end{pmatrix}[[C_{l_i}(\hat{\boldsymbol{k}}_i)\otimes C_{l'_i}(\hat{\boldsymbol{k}}_i)]^{L_i}\otimes[C_{l_f}(\hat{\boldsymbol{k}}_f)\otimes C_{l'_f}(\hat{\boldsymbol{k}}_f)]^{L_f}]^{k}_{q}. \tag{2.11}$$

Defining $T_{kq}(K,K')$,

$$T_{kq}(K,K')\equiv\frac{2-\delta_{KK'}}{2}\frac{1}{N_R}\{\mathrm{Tr}(\boldsymbol{M}_{K'}\tau_{kq}\boldsymbol{M}^{\dagger}_{K})+\mathrm{Tr}(\boldsymbol{M}_{K}\tau_{kq}\boldsymbol{M}^{\dagger}_{K'})\}, \tag{2.12}$$

and using Eqs. (2.8)–(2.11), we get $T_{kq}(K,K')$ in the coordinate system, $y\|\boldsymbol{k}_i\times\boldsymbol{k}_f$ and $z\|\boldsymbol{k}_i$,

$$T_{kq}(K,K')=(-)^{k+\Delta P}\frac{2-\delta_{K'K}}{N_R}\begin{pmatrix}\mathrm{Re}\\ i\,\mathrm{Im}\end{pmatrix}\sum_{s_is'_is_f}\hat{s}_i\hat{s}'_i\hat{s}_aW(s'_is_Aks_a;s_as_i)W(ks_iK's_f;s'_iK)\hat{K}^2\hat{K}'^2$$
$$\times\sum_{l_i=K-K}^{K}\sum_{l'_i=K'-K'}^{K'}\sum_{L_iL_f}\hat{L}_i\hat{L}_f(l_il'_i00|L_i0)(l_fl'_f00|L_f0)(L_iL_f0q|kq)$$
$$\times C_{L_fq}(\theta,\phi=0)U\begin{pmatrix} l_i & l_f & K\\ l'_i & l'_f & K'\\ L_i & L_f & k\end{pmatrix}F^*(s_is_fKl_i;\cos\theta)F(s'_is_fK'l'_i;\cos\theta), \tag{2.13}$$

where $\Delta P=0$ (1) for the no (yes) parity change and Re (i Im) in the large parentheses is for $k=$even (odd). The quantity $T_{kq}(K,K')$ is invariant under the exchange between K and K' and the factor $(2-\delta_{K'K})$ avoids double counting for $K'=K$ when employed in Eq. (2.6). From Eqs. (2.6) and (2.12), the decomposition of T_{kq} is described as

$$T_{kq}=\sum_{K\leqslant K'}T_{kq}(K,K'), \tag{2.14}$$

where K and K' are restricted by $|s_i-s_f|\leqslant K(K')\leqslant s_i+s_f$ due to Eq. (2.7), and Eq. (2.13) provides the component $T_{kq}(K,K')$, which is the analyzing power induced by the rank K amplitude and the rank K' one in the spin space.

The quantity N_R is decomposed in a similar way. The (K,K') component is given by setting $k=q=0$ in the numerator of Eq. (2.13),

$$N_R(K,K')=\delta_{K'K}(-)^{\Delta P+K}\hat{K}^2\sum_{l_i=K-K}^{K}\sum_{l'_i=K'-K'}^{K'}\sum_{L}$$
$$\times(l_il'_i00|L0)(l_fl'_f00|L0)$$
$$\times(-)^{l_i+l'_f}W(l_il_fl'_il'_f;KL)C_{L0}(\theta,\phi=0)$$
$$\sum_{s_is_f}\mathrm{Re}[F^*(s_is_fKl_i;\cos\theta)F(s_is_fKl'_i;\cos\theta)], \tag{2.15}$$

and N_R is given by

$$N_R=\sum_{K}N_R(K,K). \tag{2.16}$$

The cross section σ is proportional to N_R and the proportional factor depends on the reaction type and then will be given for each example in the following sections.

Since the present formulas are exact and model independent, in numerical analyses one can treat the amplitudes, or quantities composed of the amplitudes, as flexible parameters like phase shifts in elastic scattering. In such an approach, it is convenient to expand the amplitude by the Legendre polynomials for describing the θ dependence,

$$F(s_is_fKl_i;\cos\theta)=F_0(s_is_fKl_i)$$
$$\times\left(1+\sum_{l=1}\gamma_l(s_is_fKl_i)P_l(\cos\theta)\right), \tag{2.17}$$

TABLE I. $Q_{00,l_i l_i'}$ for $K=1$ and 2 in the cases of $\Delta P=0$ and $\Delta P\neq 0$.

$Z_{l_i l_i'}(K,K')$	$Q_{00,l_i l_i'}$ for $\Delta P=0$	$Q_{00,l_i l_i'}$ for $\Delta P\neq 0$
$Z_{00}(K,K)$	$\delta_{K,\mathrm{even}}$	$\delta_{K,\mathrm{odd}}$
$Z_{01}(1,1)$	0	$2\cos\theta$
$Z_{11}(1,1)$	$\frac{1}{2}\sin^2\theta$	1
$Z_{01}(2,2)$	$\frac{2\sqrt{2}}{\sqrt{3}}\cos\theta$	0
$Z_{11}(2,2)$	$\frac{1}{6}(\cos^2\theta+3)$	$\frac{1}{2}\sin^2\theta$
$Z_{02}(2,2)$	$3\cos^2\theta-1$	0
$Z_{12}(2,2)$	$\frac{2\sqrt{2}}{\sqrt{3}}\cos\theta$	$\cos\theta\sin^2\theta$
$Z_{22}(2,2)$	1	$\frac{1}{2}\sin^2\theta$

where $F_0(s_i s_f K l_i)$ and $\gamma_l(s_i s_f K l_i)$ are treated as adjustable parameters. For deuteron elastic scattering by spinless targets, it has been shown [5,7] that Eq. (2.7) is equivalent to the usual partial-wave expansion of scattering amplitudes when Eq. (2.17) is applied. Thus, at low energies, only few terms of small l are important in the expansion (2.17). Remembering

$$P_l(\cos\theta)=\sum_m C^*_{lm}(\hat{\boldsymbol{k}}_i)C_{lm}(\hat{\boldsymbol{k}}_f), \tag{2.18}$$

one will see that the θ dependence of $F(s_i s_f K l_i;\cos\theta)$ yields additional orbital angular momenta both in the incident and outgoing channels.

Equation (2.13) includes important information on the analyzing powers at very low energies. At such energies, the dominant partial wave is the S wave. For the S wave, $l_i=l_i'=L_i=0$ and the θ dependence of $F(s_i s_f K l_i;\cos\theta)$ is negligible. Then, we get, for $k=$ even,

$$T_{kq}(K,K')\propto P_k^q(\cos\theta), \tag{2.19}$$

where $P_k^q(\cos\theta)$ is normalized with the phase as usual. Earlier, a similar feature of T_{kq} was found by the approximation where the spin-dependent amplitude is treated in first order [7]. However, Eq. (2.13) shows that Eq. (2.19) holds without the limitation due to this approximation and is more general. In comparison with experimental data, some observed T_{2q} exhibit this characteristic; for example, in the $^2\mathrm{H}(\vec{d},p)^3\mathrm{H}$ and $^2\mathrm{H}(\vec{d},n)^3\mathrm{He}$ reactions at $E_d=30$ keV and the $^3\mathrm{He}(\vec{d},\gamma)^5\mathrm{Li}$ one at $E_d=800$ keV, the measured angular distribution of T_{2q} is approximately described by $P_2^q(\cos\theta)$ [5,7,8]. The feature of the analyzing power by Eq. (2.19) is expected to be observed when the Q value of the reaction is finite and thus the effective l_f is sufficiently large to get $L_f=k(\mathrm{even})$. In the application in the following sections, we will discuss this feature in other reactions.

TABLE II. $Q_{11,l_i l_i'}$ for $K,K'\leqslant 2$ in the case of $\Delta P=0$.

K	K'	$Y_{l_i l_i'}(K,K')$	$Q_{11,l_i l_i'}(K,K')$
1	2	$Y_{10}(1,2)$	$\sqrt{\frac{3}{2}}\sin\theta$
		$Y_{11}(1,2)$	$\cos\theta\sin\theta$
		$Y_{12}(1,2)$	$\sqrt{\frac{3}{2}}\sin\theta$
2	2	$Y_{10}(2,2)$	$-\sqrt{\frac{15}{2}}\sin\theta$
		$Y_{20}(2,2)$	$3\sqrt{5}\cos\theta\sin\theta$

Using Eqs. (2.13) and (2.15), $N_R(K,K')$, $iT_{11}(K,K')$, and $T_{2q}(K,K')$ are provided in more convenient forms for practical use. Define

$$X_{l_i l_i'}(K,K')=\sum_{s_i s_i' s_f}\hat{s}_i\hat{s}_i'\hat{s}_a W(s_i' s_A 2 s_a;s_a s_i)W \times(2 s_i K' s_f;s_i' K)\mathrm{Re}\{F^*(s_i s_f K l_i;\cos\theta)F \times(s_i' s_f K' l_i';\cos\theta)\}, \tag{2.20}$$

$$Y_{l_i l_i'}(K,K')=\sum_{s_i s_i' s_f}\hat{s}_i\hat{s}_i'\hat{s}_a W(s_i' s_A 1 s_a;s_a s_i)W \times(1 s_i K' s_f;s_i' K)\mathrm{Im}\{F^*(s_i s_f K l_i;\cos\theta)F \times(s_i' s_f K' l_i';\cos\theta)\}, \tag{2.21}$$

which satisfy, for $K'=K$,

$$X_{l_i l_i'}(K,K)=X_{l_i' l_i}(K,K),\quad Y_{l_i l_i'}(K,K)=-Y_{l_i' l_i}(K,K) \tag{2.22}$$

and

$$Z_{l_i l_i'}(K,K)=\sum_{s_i s_f}\mathrm{Re}\{F^*(s_i s_f K l_i;\cos\theta)F(s_i s_f K l_i';\cos\theta)\}. \tag{2.23}$$

Using these quantities

$$T_{2q}(K,K')=\frac{1}{N_R}\sum_{l_i=K-K}^{K}\sum_{l_i'=K'-K'}^{K'}Q_{2q,l_i l_i'} \times(K,K')X_{l_i l_i'}(K,K'), \tag{2.24}$$

$$iT_{11}(K,K')=\frac{1}{N_R}\sum_{l_i=K-K}^{K}\sum_{l_i'=K'-K'}^{K'}Q_{11,l_i l_i'} \times(K,K')Y_{l_i l_i'}(K,K'), \tag{2.25}$$

and

TABLE III. $Q_{20,l_il_i'}$, $Q_{21,l_il_i'}$, and $Q_{22,l_il_i'}$ for $K,K' \leqslant 2$ in the case of $\Delta P=0$.

K	K'	$X_{l_il_i'}(K,K')$	$Q_{20,l_il_i'}(K,K')$	$Q_{21,l_il_i'}(K,K')$	$Q_{22,l_il_i'}(K,K')$
1	1	$X_{11}(1,1)$	$\frac{\sqrt{3}}{2\sqrt{2}}\sin^2\theta$	0	$\frac{3}{4}\sin^2\theta$
1	2	$X_{10}(1,2)$	$3\sqrt{5}\cos\theta\sin^2\theta$	$\sqrt{\frac{15}{2}}(2\cos^2\theta-1)\sin\theta$	$-\sqrt{\frac{15}{2}}\cos\theta\sin^2\theta$
		$X_{11}(1,2)$	$\sqrt{\frac{15}{2}}\sin^2\theta$	$\sqrt{5}\cos\theta\sin\theta$	$-\frac{\sqrt{5}}{2}\sin^2\theta$
		$X_{12}(1,2)$	0	$\sqrt{\frac{15}{2}}\sin\theta$	0
2	2	$X_{00}(2,2)$	$-\frac{5}{\sqrt{14}}(3\cos^2\theta-1)$	$\frac{5\sqrt{3}}{\sqrt{7}}\cos\theta\sin\theta$	$-\frac{5}{2}\sqrt{\frac{3}{7}}\sin^2\theta$
		$X_{01}(2,2)$	$-\frac{5}{\sqrt{21}}\cos\theta(3\cos^2\theta+1)$	$\frac{5}{\sqrt{14}}(2\cos^2\theta+1)\sin\theta$	$-\frac{5}{\sqrt{14}}\cos\theta\sin^2\theta$
		$X_{02}(2,2)$	$-\frac{10}{\sqrt{14}}(3\cos^2\theta-1)$	$\frac{5\sqrt{3}}{\sqrt{7}}\cos\theta\sin\theta$	$\frac{5\sqrt{3}}{\sqrt{7}}\sin^2\theta$
		$X_{11}(2,2)$	$-\frac{5}{6\sqrt{14}}(5\cos^2\theta+3)$	$\frac{5}{\sqrt{21}}\cos\theta\sin\theta$	$-\frac{5\sqrt{3}}{4\sqrt{7}}\sin^2\theta$
		$X_{12}(2,2)$	$-\frac{20}{\sqrt{21}}\cos\theta$	$\frac{5}{\sqrt{14}}\sin\theta$	0
		$X_{22}(2,2)$	$-\frac{5\sqrt{2}}{7}$	0	0

$$N_R(K,K)=\sum_{l_i=K-K}^{K}\sum_{l_i'=K'-K'}^{K'}Q_{00,l_il_i'}(K,K)Z_{l_il_i'}(K,K), \tag{2.26}$$

where Q's for $K,K' \leqslant 2$ are given in Tables I–V. These Q's are different between the cases $\Delta P=0$ and $\Delta P \neq 0$ because of the difference in the available l_i due to the different $\overline{K}$. Then Q's are described for $\Delta P=0$ and $\Delta P \neq 0$, separately.

TABLE IV. $Q_{11,l_il_i'}$ for $K,K' \leqslant 2$ in the case of $\Delta P \neq 0$.

K	K'	$Y_{l_il_i'}(K,K')$	$Q_{11,l_il_i'}(K,K')$
1	1	$Y_{01}(1,1)$	$3\sin\theta$
1	2	$Y_{01}(1,2)$	$\frac{3}{\sqrt{2}}\sin\theta$
		$Y_{02}(1,2)$	$\frac{3}{\sqrt{2}}\cos\theta\sin\theta$
		$Y_{11}(1,2)$	$\frac{3}{\sqrt{2}}\cos\theta\sin\theta$
		$Y_{12}(1,2)$	$\frac{3}{\sqrt{2}}\sin\theta$
2	2	$Y_{12}(2,2)$	$\frac{\sqrt{5}}{2}\sin^3\theta$

III. APPLICATION TO THE ^{3}He$(\vec{d},p)^4$He REACTION AT THE 430-keV RESONANCE

In the ^{3}He$(\vec{d},p)^4$He reaction at the 430-keV resonance, the vector and tensor analyzing powers and some spin correlation coefficients were measured earlier [13] and the cross section data have been reported quite recently [14]. These experimental data have been analyzed by the Legendre-polynomial fit. The analyses have claimed P-wave and D-wave contributions to be important, in addition to the S-wave one which is dominant. In the following, we will reanalyze the data by using Eqs. (2.13)–(2.17) and discuss the origin of the P-wave effect.

In the reaction, the possible s_i is 1/2 and 3/2. However, experimental evidence—for example, phase shifts of p-α scattering—shows the 430-keV resonance to be the $3/2^+$ state by 99% [15]. Then we will assume the contribution of $s_i=1/2$ to be negligible. First, we will consider the S wave for the incident channel and later investigate the contribution of the P waves. For the S wave, because of $s_i=3/2$ and $s_f=1/2$, the reaction takes place by tensor interactions which include effects of the D states of the internal motions of the deuteron, ^{3}He and ^{4}He. Because of the S-wave restriction, the vector analyzing power vanishes. The tensor analyzing powers from the tensor interaction are given by $X_{00}(2,2)$ multiplied by $Q_{2q00}(2,2)$ in Table III. The Racah coefficients in $X_{00}(2,2)$ are evaluated with the specifications, $s_a=1$ and $s_A=1/2$ and the factor $|F(\frac{3}{2}\frac{1}{2}20;\cos\theta)|^2$ is canceled by the denominator N_R which is $Z_{00}(2,2)$ because $Q_{0000}(2,2)=1$ as in Table I. Finally we get

TABLE V. $Q_{20,l_il_i'}$, $Q_{21,l_il_i'}$, and $Q_{22,l_il_i'}$ for $K,K' \leqslant 2$ in the case of $\Delta P \neq 0$.

K	K'	$X_{l_il_i'}(K,K')$	$Q_{20,l_il_i'}(K,K')$	$Q_{21,l_il_i'}(K,K')$	$Q_{22,l_il_i'}(K,K')$
1	1	$X_{00}(1,1)$	$-\sqrt{\frac{3}{2}}(3\cos^2\theta-1)$	$3\cos\theta\sin\theta$	$-\frac{3}{2}\sin^2\theta$
		$X_{01}(1,1)$	$-2\sqrt{6}\cos\theta$	$3\sin\theta$	0
		$X_{11}(1,1)$	$-\sqrt{6}$	0	0
1	2	$X_{01}(1,2)$	$\sqrt{15}\cos\theta\sin^2\theta$	$\sqrt{\frac{5}{2}}(2\cos^2\theta-1)\sin\theta$	$-\sqrt{\frac{5}{2}}\cos\theta\sin^2\theta$
		$X_{02}(1,2)$	$\sqrt{15}\sin^2\theta$	$\sqrt{\frac{5}{2}}\cos\theta\sin\theta$	$\sqrt{\frac{5}{2}}\sin^2\theta$
		$X_{11}(1,2)$	0	$\sqrt{\frac{5}{2}}\cos\theta\sin\theta$	$-\sqrt{10}\sin^2\theta$
		$X_{12}(1,2)$	0	$\sqrt{\frac{5}{2}}\sin\theta$	0
2	2	$X_{11}(2,2)$	$-\frac{5}{2\sqrt{14}}(3\cos^2\theta-2)\sin^2\theta$	$\frac{15}{2\sqrt{21}}\cos\theta\sin^3\theta$	$\frac{15}{4\sqrt{21}}\cos^2\theta\sin^2\theta$
		$X_{12}(2,2)$	$-\frac{5}{\sqrt{14}}\cos\theta\sin^2\theta$	$\frac{15}{2\sqrt{21}}\sin^3\theta$	$\frac{15}{2\sqrt{21}}\cos\theta\sin^2\theta$
		$X_{22}(2,2)$	$-\frac{5}{2\sqrt{14}}\sin^2\theta$	0	$\frac{15}{4\sqrt{21}}\sin^2\theta$

$$T_{2q} = -\frac{1}{\sqrt{5}}P_2^q(\cos\theta) \quad \text{for } q=0,1,2. \tag{3.1}$$

This exhibits what we predicted by Eq. (2.19) and is also equivalent to the result in Ref. [10]. The analyzing-power data are in Ref. [13], where the twice analyzing powers are given except for T_{20} [16]. We will follow this scale. Figure 1 shows the comparison between the calculated by Eq. (3.1) and the experimental data, where the calculation gives considerably good agreement with the data of T_{20}, T_{21}, and T_{22}, both in magnitude and angular shape. This indicates that the contribution of the transition from the S wave by the tensor interaction is dominant. However, small but systematic differences are observed between the calculation and the experiment. To describe the differences more clearly, we will define ΔT_{2q} as

$$\Delta T_{2q} = T_{2q} + \frac{1}{\sqrt{5}}P_2^q(\cos\theta), \tag{3.2}$$

which we will study by including corrections due to transitions from the P wave, allowing the admixture of negative-parity states—for example, a $3/2^-$ one [17]—at 430 keV.

For the P-wave effect, we will take account of contributions of the vector amplitudes in addition to those of the tensor ones. Since the reaction occurs dominantly by the tensor interaction, the vector amplitude is considered only by the interference term with the tensor amplitudes. Then, the P-wave contributions are given by the terms of tensor amplitudes, $X_{01}(2,2)$ and $X_{11}(2,2)$, and those of the tensor-vector interference, $X_{10}(1,2)$ and $X_{11}(1,2)$, for which Q's are given in Table III. Calculate the Racah coefficients included and define the relative magnitudes of the P-wave amplitudes to the S-wave one by

$$\begin{pmatrix} p_T \\ q_T \end{pmatrix} = \begin{pmatrix} \mathrm{Re} \\ \mathrm{Im} \end{pmatrix} \left[F^*\left(\frac{3}{2}\frac{1}{2}20;\cos\theta\right) F\left(\frac{3}{2}\frac{1}{2}21;\cos\theta\right) \right] \Big/ N_R(S), \tag{3.3}$$

$$p_T' = \left| F\left(\frac{3}{2}\frac{1}{2}21;\cos\theta\right) \right|^2 \Big/ N_R(S), \tag{3.4}$$

$$\begin{pmatrix} p_V \\ q_V \end{pmatrix} = \begin{pmatrix} \mathrm{Re} \\ \mathrm{Im} \end{pmatrix} \left[F^*\left(\frac{3}{2}\frac{1}{2}11;\cos\theta\right) F\left(\frac{3}{2}\frac{1}{2}20;\cos\theta\right) \right] \Big/ N_R(S), \tag{3.5}$$

$$\begin{pmatrix} p_V' \\ q_V' \end{pmatrix} = \begin{pmatrix} \mathrm{Re} \\ \mathrm{Im} \end{pmatrix} \left[F^*\left(\frac{3}{2}\frac{1}{2}11;\cos\theta\right) F\left(\frac{3}{2}\frac{1}{2}21;\cos\theta\right) \right] \Big/ N_R(S), \tag{3.6}$$

with

$$N_R(S) \equiv \left| F\left(\frac{3}{2}\frac{1}{2}20;\cos\theta\right) \right|^2, \tag{3.7}$$

where p's are for the cross section and the tensor analyzing powers and q's for the vector analyzing power. We get the tensor analyzing powers as

$$T_{20}=\frac{1}{\overline{N}_R}\left\{-\frac{1}{2\sqrt{2}}(3\cos^2\theta-1)-\frac{1}{2\sqrt{3}}p_T\cos\theta(3\cos^2\theta+1)-\frac{1}{12\sqrt{2}}p'_T(5\cos^2\theta+3)-\frac{3}{2}p_V\cos\theta\sin^2\theta-\frac{3}{2\sqrt{6}}p'_V\sin^2\theta\right\}, \tag{3.8}$$

$$T_{21}=\frac{1}{\overline{N}_R}\left\{\frac{\sqrt{3}}{2}\cos\theta\sin\theta+\frac{1}{2\sqrt{2}}p_T(2\cos^2\theta+1)\sin\theta+\frac{1}{2\sqrt{3}}p'_T\cos\theta\sin\theta-\frac{\sqrt{3}}{2\sqrt{2}}p_V(2\cos^2\theta-1)\sin\theta-\frac{1}{2}p'_V\cos\theta\sin\theta\right\}, \tag{3.9}$$

$$T_{22}=\frac{1}{\overline{N}_R}\left\{-\frac{\sqrt{3}}{4}\sin^2\theta-\frac{1}{2\sqrt{2}}p_T\cos\theta\sin^2\theta-\frac{\sqrt{3}}{8}p'_T\sin^2\theta+\frac{\sqrt{3}}{2\sqrt{2}}p_V\cos\theta\sin^2\theta+\frac{1}{4}p'_V\sin^2\theta\right\}, \tag{3.10}$$

with

$$\overline{N}_R=1+\frac{2\sqrt{2}}{3}p_T\cos\theta+\frac{1}{6}p'_T(\cos^2\theta+3), \tag{3.11}$$

which are obtained by the terms of $Z_{00}(2,2)$, $Z_{01}(2,2)$, and $Z_{11}(2,2)$ with the related Q's in Table I. The first term of each T_{2q} in Eqs. (3.8)–(3.10) describes the S wave contribution by the tensor interaction, Eq. (3.1), when $\overline{N}_R=1$. The P-wave corrections due to the tensor amplitudes are denoted by the coefficients p_T and p'_T, and those due to the tensor-vector interference terms are by p_V and p'_V. Since these p's are expected to have small magnitudes, we will neglect the correction by the θ dependence of the amplitudes and treat p's as the θ-independent parameters. In Figs. 2 and 3, the tensor P-wave contributions and the tensor-vector interference P-wave ones, which are calculated by Eqs. (3.8)–(3.11), are compared with the empirical ΔT_{2q} which are obtained by using the observed T_{2q} on the right-hand side (RHS) of Eq. (3.2). The order of magnitude of p's is assumed to be 0.1 as in Table VI, considering the P-wave effects to be small corrections compared to the S-wave contribution. In Fig. 2, the p_T terms with $p_T=0.1$ almost fit the data of ΔT_{20} but fail to reproduce those of $2\Delta T_{21}$ at large angles and give too small $2\Delta T_{22}$ compared to the data except those at angles around $\theta=90°$. Such unsuccessful results are not improved by varying the magnitude and/or changing the sign of p_T. That is, the p_T term cannot reproduce all of ΔT_{2q} simultaneously. As seen in the figure, a similar consideration excludes the possibility of explaining the ΔT_{2q} data by the p'_T effects or a combination of the p_T and p'_T effects. On the other hand, as is shown in Fig. 3, the p_V effects with $p_V=0.07$ reproduce the global features of ΔT_{2q} data for $q=0$, 1, and 2 simultaneously although several data points—for example, two data points of $2\Delta T_{21}$ around $\theta=90°$—deviate from the calculated curves. The contributions of the p'_V terms with $p'_V=-0.05$ seem to improve the agreement with the data but the improvement is not quite sure. The agreement with the data of $2\Delta T_{21}$ becomes worse by including the p'_V terms around $\theta=120°$. From these analyses, it will be concluded that the data of ΔT_{2q} are explained by the P-wave effects, which are mainly produced by the interference between the S-wave amplitude by the tensor interactions and the P-wave one by the vector interactions. In the present reaction, the vector interaction will be interpreted as spin-orbit interactions. Because of the very low incident energy, the spin-orbit interaction will be very weak in the incident channel. On the other hand, the large $p-\alpha$ kinetic energy due to the high Q value in the outgoing channel produces a strong p-α spin-orbit interaction, which will be responsible for such P-wave effects.

The cross section σ is given by

$$\sigma=\frac{\mu_i\mu_f k_f}{24\pi^2 k_i}\left|F\left(\frac{3}{2}\frac{1}{2}20;\cos\theta\right)\right|^2\overline{N}_R, \tag{3.12}$$

where μ_i (μ_f) is the reduced mass in the incident (outgoing) channel and $\overline{N}_R$ is given by Eq. (3.11). From the analyses of ΔT_{2q} stated above, one can choose $p_T=p'_T=0$ and then $\overline{N}_R=1$. We will apply the Legendre-polynomial expansion (2.17) to $F(\frac{3}{2}\frac{1}{2}20;\cos\theta)$ up to $l=1$ and get

$$\sigma=\sigma_0(1+\gamma_1\cos\theta)^2, \tag{3.13}$$

where

$$\sigma_0=\frac{\mu_i\mu_f k_f}{24\pi^2 k_i}\left|F_0\left(\frac{3}{2}\frac{1}{2}20\right)\right|^2. \tag{3.14}$$

In Fig. 4(a), Eq. (3.13) is compared to the experimental data [14] with $\sigma_0=62.0$ mb/sr and $\gamma_1=0.018$ (see Table VII). The calculation reproduces most of the data. However, several data points, particularly at forward angles, deviate from the theoretical curve. When this discrepancy is assumed to be unimportant, the anisotropy of the cross section will be explained as the contribution of the γ_1 term which describes

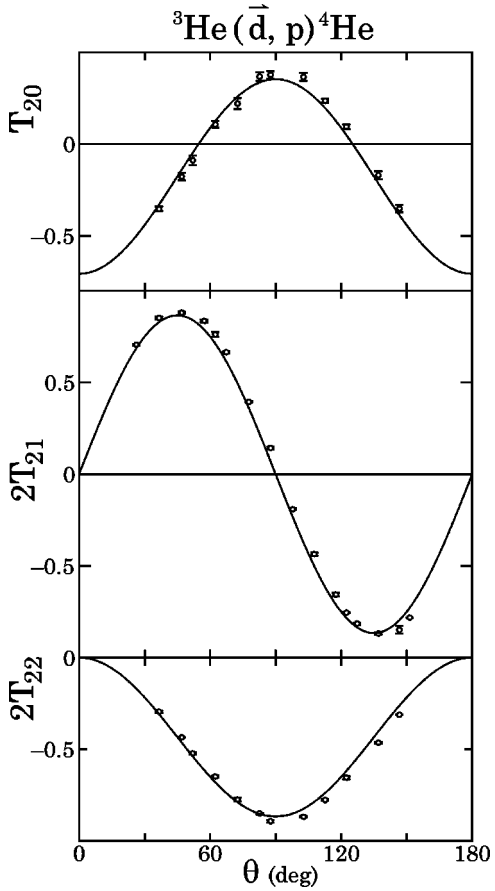

FIG. 1. Tensor analyzing powers in the $^3\mathrm{He}(\vec{d},p)^4\mathrm{He}$ reaction at the 430-keV resonance. The solid lines represent the calculation by the S-wave assumption, $T_{2q}=(-1/\sqrt{5})P_2^q(\cos\theta)$ with $q=0,1,2$. The experimental data are taken from Ref. [13]. The quantities T_{21} and T_{22} are given in the double scale.

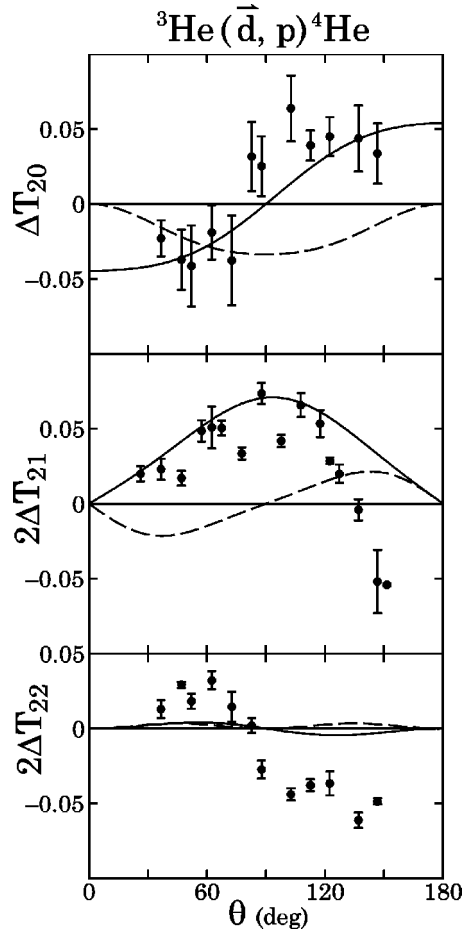

FIG. 2. P-wave corrections due to tensor interactions to tensor analyzing powers in the $^3\mathrm{He}(\vec{d},p)^4\mathrm{He}$ reaction at the 430-keV resonance. The solid lines are calculated by set A in Table VI and describe the contribution of the interference terms between the S wave and P wave. The dashed lines calculated by set B are for the pure P-wave contributions. The data of ΔT_{2q} are obtained by $\Delta T_{2q}=T_{2q}(\mathrm{measured})+(1/\sqrt{5})P_2^q(\cos\theta)$. ΔT_{21} and ΔT_{22} are given in the double scale. The measured T_{2q} are taken from Ref. [13].

the P-wave effect due to the tensor interaction. Such a small magnitude of γ_1 will justify the neglect of the θ dependence of p's in the analyses of the tensor analyzing powers.

The vector analyzing power iT_{11} is given by the terms of $Y_{10}(2,2)$, $Y_{10}(1,2)$, and $Y_{11}(1,2)$ with the related Q's in Table II. Calculating the Racah coefficients, we get

$$iT_{11}=\frac{\beta_{d+^3\mathrm{He}}}{1+\gamma_1\cos\theta}\sin\theta+\frac{\beta'_{d+^3\mathrm{He}}}{(1+\gamma_1\cos\theta)^2}\cos\theta\sin\theta, \tag{3.15}$$

with

$$\beta_{d+^3\mathrm{He}}=\frac{3}{2\sqrt{2}}q_T-\frac{1}{2\sqrt{6}}q_V,\quad \beta'_{d+^3\mathrm{He}}=-\frac{1}{6}q'_V, \tag{3.16}$$

where the θ dependence of the invariant amplitudes is considered only for the main amplitude $F(\frac{3}{2}\frac{1}{2}20;\cos\theta)$. In Fig. 4(b), the vector analyzing powers calculated with $q_V=-0.09$ and $q_T=0$ are compared with the experimental data [13], choosing $q'_V=0$, 0.09, and 0.14. The contribution of finite q'_V shifts the maximum of iT_{11} toward larger angles, reproducing the feature of the observed angular distribution. Then the spin-orbit interaction will be important to fit the data of the vector analyzing power.

IV. APPLICATION TO $^1\mathrm{H}(\vec{d},\gamma)^3\mathrm{He}$ REACTIONS BELOW 80 keV

Since the spin parity of a photon is 1^-, $^1\mathrm{H}(\vec{d},\gamma)^3\mathrm{He}$ reactions are typical examples of the case where the parity of the system is changed by the reaction. Because of scarce experimental data at very low energies, we will treat the simple case where only the vector amplitudes are effective. This treatment takes account of the most important mechanism of the reaction, since the emission of the photon takes place essentially due to the vector interaction which is proportional to the polarization vector of the photon. More details of the interaction will be discussed at the end of this section.

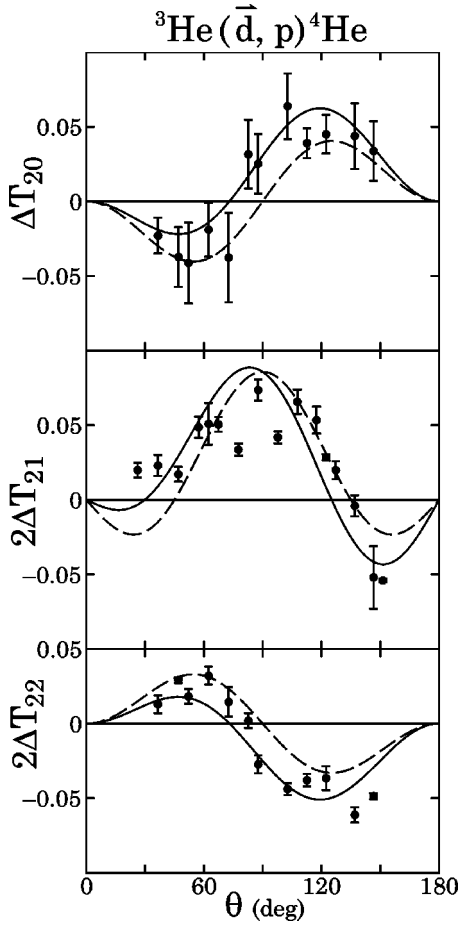

FIG. 3. *P*-wave corrections due to interference between the vector amplitude and the tensor one to tensor analyzing powers in the ^{3}He($\vec{d}$,p)^{4}He reaction at the 430-keV resonance. The dashed lines are calculated by the parameter set *C* in Table VI and represent the contribution of the interference terms between the *S*-wave transition due to tensor interactions and the *P*-wave one due to vector interactions. The solid lines calculated by set *D* include the additional contributions from the interference between the *P*-wave transition due to tensor interactions and the *P*-wave one due to vector interactions. The definition and scale of ΔT_{2q} are the same as those in Fig. 2. The data are taken from Ref. [13].

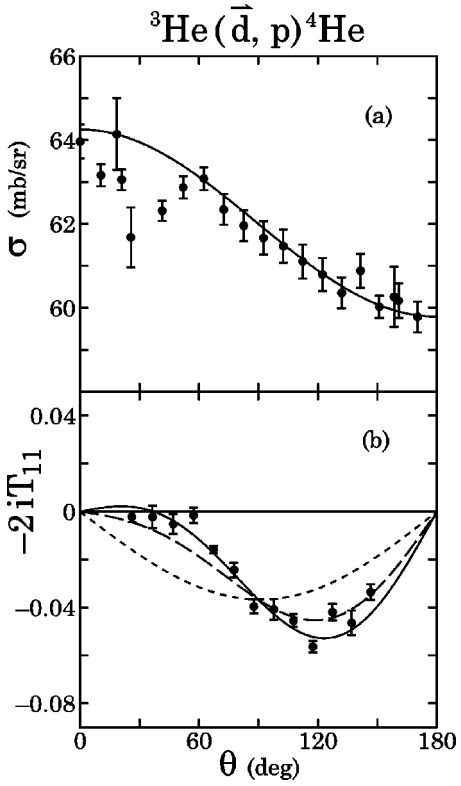

FIG. 4. Cross section and vector analyzing power in the ^{3}He($\vec{d}$,p)^{4}He reaction at the 430-keV resonance. (a) The cross section σ calculated by the parameters in Table VII (solid line) is compared with the experimental data in Ref. [14]. (b) The vector analyzing power iT_{11} calculated by the interference terms between the tensor amplitude and the vector one is compared with the experimental data in Ref. [13], where the twice analyzing power with the negative sign is given. The dotted, dashed, and solid lines are calculated by sets *A*, *B*, and *C* in Table VII, respectively.

For the vector amplitudes, the cross section is given by $N_R(1,1)$ which consists of the terms of $Z_{00}(1,1)$, $Z_{01}(1,1)$, and $Z_{11}(1,1)$ with the corresponding Q's in Table I,

$$\sigma = \frac{\mu_i k_f^2}{24\pi^2 c k_i} N_R(1,1), \tag{4.1}$$

where

$$N_R(1,1) = \sum_{s_i s_f} \{|F(s_i s_f 10;\cos\theta)|^2 + |F(s_i s_f 11;\cos\theta)|^2 + 2\cos\theta\,\mathrm{Re}[F^*(s_i s_f 10;\cos\theta)F(s_i s_f 11;\cos\theta)]\}. \tag{4.2}$$

Experimental data are given by a kind of average over the incident energies below 80 keV and then the quality of the theoretical parameters obtained by fitting the data will necessarily be approximate. From this viewpoint, we will consider the θ dependence of the amplitudes only for the incident *S* waves for simplicity, and the θ dependence is assumed to be independent of s_i and s_f. Taking the expansion (2.17) up to $l=2$,

$$F(s_i s_f 10;\cos\theta) = F_0(s_i s_f 10) f(\theta), \tag{4.3}$$

with

$$f(\theta) = 1 + \gamma_1 P_1(\cos\theta) + \gamma_2 P_2(\cos\theta),$$

TABLE VI. Parameters used in calculations of the ^{3}He($\vec{d}$,p)^{4}He reaction for tensor analyzing powers.

	p_T	p'_T	p_V	p'_V
A	0.1	0	0	0
B	0	0.1	0	0
C	0	0	0.07	0
D	0	0	0.07	−0.05

TABLE VII. Parameters used in calculations of the $^3\mathrm{He}(\vec{d},p)^4\mathrm{He}$ reaction for cross section and vector analyzing power.

σ_0		62.0 mb/sr	
γ_1		0.018	
q_V		−0.09	
	A	B	C
q'_V	0	0.09	0.14

and defining

$$a \equiv \sum_{s_i s_f} \{|F_0(s_i s_f 10)|^2 + |F_0(s_i s_f 11)|^2\}, \tag{4.4}$$

$$b \equiv \sum_{s_i s_f} \mathrm{Re}[F_0^*(s_i s_f 10) F_0(s_i s_f 11)], \tag{4.5}$$

and

$$\sigma_0 = \frac{\mu_i k_f^2}{24\pi^2 c k_i} a, \tag{4.6}$$

we get

$$\sigma = \sigma_0 f(\theta)\left(f(\theta) + \frac{2b}{a}\cos\theta \right). \tag{4.7}$$

The vector analyzing power iT_{11} is given by $Y_{01}(1,1)$ with $Q_{11,01}(1,1)$ in Table IV,

$$iT_{11} = \frac{3}{N_R(1,1)} Y_{01}(1,1)\sin\theta. \tag{4.8}$$

Defining β_{d+p},

$$\beta_{d+p} \equiv \frac{3Y_{01}(1,1)}{a f(\theta)}, \tag{4.9}$$

which is θ independent because the θ dependence of $Y_{01}(1,1)$ is canceled by that of the denominator, we get

$$iT_{11} = \beta_{d+p} \frac{1}{f(\theta) + \frac{2b}{a}\cos\theta} \sin\theta. \tag{4.10}$$

The tensor analyzing power T_{20} is given by the use of Q's in Table V as

$$T_{20} = -\frac{1}{N_R(1,1)}\left\{ \sqrt{\frac{3}{2}}(3\cos^2\theta - 1) X_{00}(1,1) + 2\sqrt{6}\cos\theta X_{01}(1,1) + \sqrt{6} X_{11}(1,1) \right\}, \tag{4.11}$$

where the term of $X_{00}(1,1)$ describes the S-wave contribution, that of $X_{01}(1,1)$ the interference between the S wave and P wave, and the last one, $\sqrt{6}X_{11}(1,1)$, the P-wave contribution. Define the θ-independent parameters, α, ε_1, and ε_2 as

$$\alpha \equiv \frac{3X_{00}(1,1)}{2a f(\theta)^2}, \quad \varepsilon_1 \equiv \frac{X_{01}(1,1)}{X_{00}(1,1)} f(\theta),$$

$$\varepsilon_2 \equiv \frac{X_{11}(1,1)}{X_{00}(1,1)} f(\theta)^2. \tag{4.12}$$

We get

$$T_{20} = -\sqrt{\frac{2}{3}} \frac{\alpha}{1 + \frac{2b}{a}\frac{\cos\theta}{f(\theta)}} \times \left\{ (3\cos^2\theta - 1) + 4\varepsilon_1 \frac{\cos\theta}{f(\theta)} + \frac{2\varepsilon_2}{f(\theta)^2} \right\}. \tag{4.13}$$

The parameters b/a, γ_1, and γ_2 are determined by fitting the data of the cross section, while σ_0 is arbitrary because the absolute magnitude of the cross section has not been measured. We get several acceptable sets of parameters for $0 < |b/a| < 0.5$, among which the two typical ones, A and B, are given in Table VIII. Using these sets, we determine other parameters so as to reproduce the data of iT_{11} and T_{20}, for which large magnitudes of b/a give worse agreements with the data.

TABLE VIII. Parameters used in calculations of cross section and vector and tensor analyzing powers of $^1\mathrm{H}(\vec{d},\gamma)^3\mathrm{He}$ reactions.

	σ_0	b/a	γ_1	γ_2	α	ε_1	ε_2	β_{d+p}
A	1.00	−0.10	0.10	−0.40	−0.13	−0.13	0.15	−0.10
B	1.00	0.10	−0.10	−0.40	−0.13	−0.13	0.15	−0.10

The comparison of the calculations by sets A and B with the experimental data [11,18] is shown in Fig. 5, where the calculations reproduce the data reasonably well, although set B gives too small T_{20} at $\theta = 0°$. In Fig. 6, we show the theoretical prediction of T_{21} and T_{22} by sets A and B. The formulas of the analyzing powers are given by the terms of $X_{00}(1,1)$ and $X_{01}(1,1)$ with the related Q's in Table V,

$$T_{21} = \frac{2\alpha}{1 + \frac{2b}{a}\frac{\cos\theta}{f(\theta)}} \left\{ \cos\theta\sin\theta + \varepsilon_1 \frac{\sin\theta}{f(\theta)} \right\} \tag{4.14}$$

and

$$T_{22} = -\frac{\alpha}{1 + \frac{2b}{a}\frac{\cos\theta}{f(\theta)}} \sin^2\theta. \tag{4.15}$$

The experimental data in a preliminary report [18] are also given in the figure. The calculations reproduce most of the data, although T_{21} by set B is too large compared with the

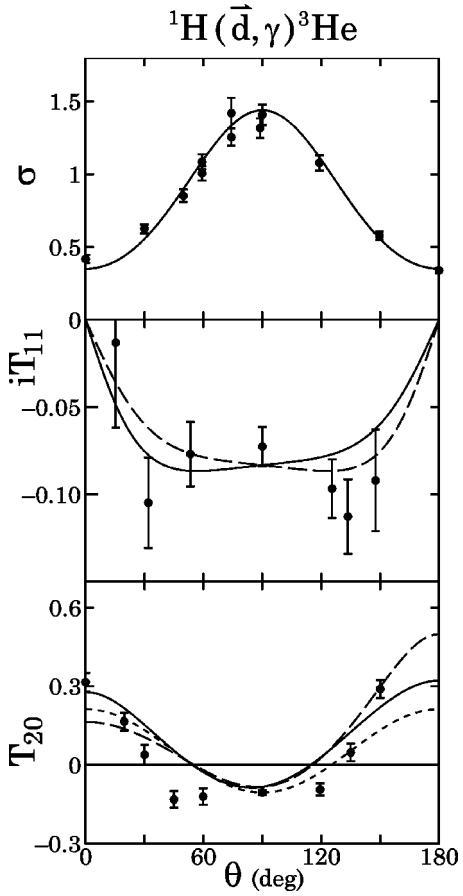

FIG. 5. Cross section and vector and tensor analyzing powers in ^{1}H($\vec{d},\gamma$)^{3}He reactions at energies below 80 keV. The calculations of σ, iT_{11}, and T_{20} by the vector amplitudes are compared with the experimental data in Refs. [11,18]. The parameters are given in Table VIII and the calculations by set A (B) are described by the solid (dashed) lines. The dashed line in σ completely overlaps the solid one. The dotted line shows $-\sqrt{\frac{16}{15}}\alpha P_2^0(\cos\theta)$.

data at $\theta=135°$. Further examinations of the theoretical prediction require more experimental data of T_{21} and T_{22}.

Now let us examine the contribution of the S wave. Keeping only the S-wave contributions, one gets, from Eqs. (4.13)–(4.15),

$$T_{2q}=-\sqrt{\frac{16}{15}}\alpha P_2^q(\cos\theta), \tag{4.16}$$

which is equivalent to our prediction, Eq. (2.19). In Figs. 5 and 6, Eq. (4.16) is compared with the experimental data, where the global features of the data of T_{20}, T_{21}, and T_{22} are simultaneously described by the single formula (4.16). The anisotropy of the angular distribution of the measure cross section is reproduced by including the P-wave contributions in addition to the S-wave one where the θ dependence of the amplitude is considered. The significance of the S-wave and P-wave contributions is consistent with the situation in recent microscopic calculations [11,19], where both $M1$ and $E1$ transitions are important. However, in the tensor analyzing powers—for example, T_{20}—the contributions of the P wave through N_R are considerably canceled by the effect of the θ dependence of $X_{00}(1,1)$ and the contributions of $X_{01}(1,1)$ and $X_{11}(1,1)$, resulting in a good description of the analyzing powers by Eq. (4.16).

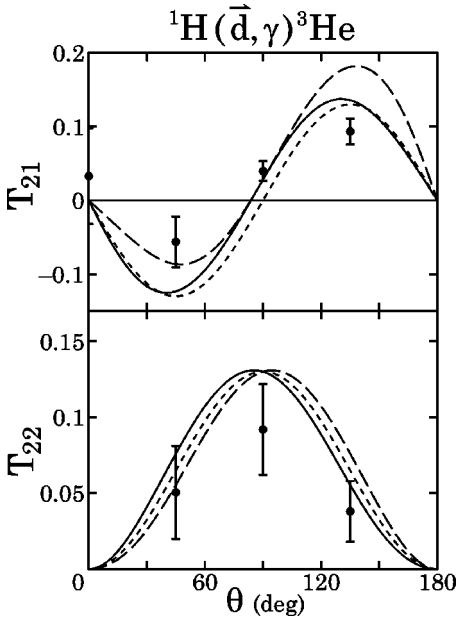

FIG. 6. Comparison of theoretical prediction of T_{21} and T_{22} with the experimental data [18] in ^{1}H($\vec{d},\gamma$)^{3}He reactions at energies below 80 keV. The calculation by the vector amplitudes are shown for the parameter set A (B) in Table VIII by the solid (dashed) lines. The dotted lines show $-\sqrt{\frac{16}{15}}\alpha P_2^1(\cos\theta)$ for T_{21} and $-\sqrt{\frac{16}{15}}\alpha P_2^2(\cos\theta)$ for T_{22}.

The present analyses explain the ^{1}H($\vec{d},\gamma$)^{3}He data successfully by the assumption of the vector-amplitude dominance. Let us consider the interactions in their first order. Both of S and D states in the internal motions of the deuteron and ^{3}He produce the vector amplitudes due to the vector property of the photon emission operator. However, the D states can produce the transition amplitudes of $K=2$ and 3. These effects should be taken into account in the calculation. Such calculations will be performed when refined experimental data become available, to avoid ambiguities due to the increase of parameters.

The present approach is of a phenomenological nature to provide information on the role of the spin-dependent interaction and the reaction mechanism in a manner independent of the details of the interactions and thus free from their ambiguities. This has different features from the conventional one such as microscopic calculations which specify the details of the interactions. Despite the difference in the approach, σ and T_{20} by the present calculation are close to those by sophisticated microscopic calculations [19] and both calculations have almost similar qualities in agreement with the experimental data. This will mean the assumption of vector-amplitude dominance employed in the calculation to be a plausible one.

V. SUMMARY AND DISCUSSIONS

The present paper derives the general formulas of the analyzing powers for $A(\vec{a},b)B$ reactions by the decomposition

of the analyzing power by the tensor rank in the spin space, using the invariant-amplitude method. From the formulas, we find that the angular distribution of T_{kq} $(k=\text{even})$ is given by $P_k^q(\cos\theta)$ when the incident beam is the S wave and the Q value has a suitable magnitude. This prediction describes the main feature of the observed analyzing powers in low energy reactions.

The explicit forms of the vector and tensor analyzing powers are given for the low tensor ranks $K=1$ and 2. They are successful in the analyses of the experimental data of the $^3\text{He}(\vec{d},p)^4\text{He}$ reaction at the 430-keV resonance and $^1\text{H}(\vec{d},\gamma)^3\text{He}$ reactions at center-of-mass energies below 80 keV. In the former, the dominant contribution to the cross section and the tensor analyzing powers arises from the S-wave transition by the tensor interactions and the observed angular distributions of tensor analyzing powers are described approximately by $P_2^q(\cos\theta)$ as was mentioned above. The deviations of the data of the tensor analyzing powers from the S-wave prediction as well as the finite vector analyzing power are explained by the P-wave corrections, for which the vector interactions in the spin space are responsible. This suggests important contributions of the p-α spin-orbit interaction in the final state. In the $^1\text{H}(\vec{d},\gamma)^3\text{He}$ reaction, the experimental data of the cross section and the vector and tensor analyzing powers are reproduced by the vector amplitudes in the spin space. The observed angular distributions of T_{2q} $(q=0,1,2)$ are approximately described by a simple form $P_2^q(\cos\theta)$.

In the present analyses, the angular distributions of the analyzing powers are due to the following two sources: $Q_{kq,l_i l_i'}(K,K')$, which originates from the geometrical part of the matrix element of $\boldsymbol{R}_{K\kappa}$, and the θ dependence of the invariant amplitude $F(s_i s_f K l_i;\cos\theta)$. In particular, the former plays essential roles in reproducing the analyzing-power data in the $^3\text{He}(\vec{d},p)^4\text{He}$ reaction. Such effects have not been recognized in conventional treatments.

Finally, considering the success of the present analyses, we hope more experimental data at low energies will become available in the future. The parameters obtained by the present theory will be useful information for calculations by models.

The authors would like to express their thanks to Professor S. Ishikawa for valuable discussions.

[1] M. Tanifuji and K. Yazaki, Prog. Theor. Phys. **40**, 1023 (1968).
[2] D. J. Hooton and R. C. Johnson, Nucl. Phys. **A175**, 583 (1971).
[3] Y. Sakuragi, M. Yahiro, M. Kamimura, and M. Tanifuji, Nucl. Phys. **A480**, 361 (1988).
[4] Y. Iseri, H. Kameyama, M. Kamimura, M. Yahiro, and M. Tanifuji, Nucl. Phys. **A490**, 383 (1988).
[5] M. Tanifuji, Phys. Lett. B **289**, 233 (1992), and references therein.
[6] M. Tanifuji, Phys. Lett. B **363**, 151 (1995).
[7] M. Tanifuji and H. Kameyama, Nucl. Phys. **A602**, 1 (1996).
[8] E. Uzu, H. Kameyama, S. Oryu, and M. Tanifuji, Few-Body Syst. **22**, 65 (1997).
[9] M. Tanifuji, S. Ishikawa, and Y. Iseri, Nucl. Instrum. Methods Phys. Res. A **402**, 433 (1998); Phys. Rev. C **57**, 2493 (1998).
[10] F. Seiler and E. Baumgartner, Nucl. Phys. **A153**, 193 (1970).
[11] G. J. Schmid, B. J. Rice, R. M. Chasteler, M. A. Godwin, G. C. Kiang, L. L. Kiang, C. M. Laymon, R. M. Prior, D. R. Tilley, and H. R. Weller, Phys. Rev. C **56**, 2565 (1997).
[12] G. G. Ohlsen, Rep. Prog. Phys. **35**, 717 (1972).
[13] Ch. Leemann, H. Bürgisser, P. Huber, U. Rohrer, H. Paetz gen Shieck, and F. Seiler, Helv. Phys. Acta **44**, 141 (1971).
[14] C. R. Brune, W. H. Geist, H. J. Karwowski, and E. J. Ludwig, TUNL **36**, 49 (1996–1997).
[15] W. Haeberli, *Nuclear Spectroscopy and Reactions*, edited by J. Cerny (Academic, New York, 1974), p. 185.
[16] R. Garrett and W. Lindstrom, Nucl. Phys. **A224**, 186 (1974).
[17] M. P. Rekalo and E. Tomasi-Gustafsson, Phys. Rev. C **57**, 2870 (1998).
[18] R. S. Canon, M. A. Godwin, J. H. Kelley, R. M. Prior, B. J. Rice, M. Spraker, D. R. Tilley, H. R. Weller, and E. A. Wulf, TUNL **37**, 55 (1997–1998).
[19] M. Viviani, R. Schiavilla, and A. Kievsky, Phys. Rev. C **54**, 534 (1996); G. Schmid *et al.*, Phys. Rev. Lett. **76**, 3088 (1996).